CrossMark

ORIGINAL PAPER

Chromium(VI) adsorption from aqueous solution by prepared biochar from *Onopordom Heteracanthom*

S. Ghorbani-Khosrowshahi[1] · M. A. Behnajady[1]

Abstract In this research, the stems of *Onopordom Heteracanthom* which is a kind of weed were converted to biochar particles, and their characteristics were investigated. The morphology and purity of these particles were examined by SEM and EDX techniques, respectively. Specific surface area was obtained as 5.73 m^2 g^{-1} by BET method. The biochar particles obtained from *Onopordom Heteracanthom* were evaluated as an adsorbent to remove Cr(VI) from aqueous environments. The effect of some parameters such as initial concentration of Cr(VI), dosage of adsorbent, and pH were investigated on the adsorption capacity of Cr(VI) onto the adsorbent. The equilibrium data were analyzed by various isotherm models. The results revealed that in this process, the adsorption isotherm and kinetics have more conformity with Langmuir isotherm and pseudo-second-order kinetics, respectively. The multi-linearity of the Weber and Morris adsorption kinetic model indicates that the intra-particle diffusion is not merely the rate-controlling step for the whole adsorption process.

Keywords Adsorption · Biochar · Cr(VI) · *Onopordom Heteracanthom*

Introduction

All over the world, the pollution of water resources has increased due to the disposal of heavy metals. Removing heavy metals from water and wastewaters as a result of industrialization has turned out to be a serious problem. Discharging of metals into water resources is one of the most critical issues regarding pollution which may have negative effects on the quality of water supply. Increasing concentrations of heavy metals in water resources have negative effects on the quality of water and have caused severe threats to the health of humankind, which are mainly related to their non-degradability and toxicity (Gode et al. 2008).

There are different heavy metals such as Cd, Cu, Zn, Ni, and Cr(VI) in surface waters (Behnajady and Bimeghdar 2014; Hu et al. 2005). Chromium has a broad usage in industry due to its strong crystalline structure, corrosion resistance, and yellow color. It is one of the essential materials in electroplating industries, tanneries, paint and pigments, wood preservation, and alloy making processes (Gupta and Babu 2009).

The toxicity of hexavalent chromium is 500 times more than the trivalent form due to its carcinogenic and mutagenic effects. Human toxicity of Cr(VI) includes skin irritation to lung cancer, as well as kidney, liver, and gastric damage (Das and Vinodhini 2010; Kotas and Stasicka 2000).

Several treatment techniques have been used for the removal of Cr(VI) from wastewater; this includes techniques such as membrane separation (Bhowal et al. 2012), electrocoagulation (Zongo et al. 2009), solvent extraction (Venkateswaran and Palanivelu 2004), reduction (An et al. 2014), reverse osmosis (Chun et al. 2004), adsorption (Behnajady and Bimeghdar 2014), and photoreduction (Behnajady et al. 2012).

However, most of these methods not only are expensive but also have many disadvantages such as incomplete metal removal, high reagent, and energy requirements (Aliabadi et al. 2006; Gupta and Babu 2009). In order to

✉ M. A. Behnajady
  behnajady@gmail.com

[1] Department of Chemistry, Tabriz Branch, Islamic Azad University, Tabriz, Iran

Springer

achieve complete removal of the metals, adsorption can be remarked as a proper procedure with low usage of chemicals and energy. It can be a suitable and effective low-cost method for separating heavy metals from aqueous phase if a low-cost and effective adsorbent has been used (Bailey et al. 1999).

Despite of the fact that adsorption by activated carbon is a major technique for removing toxic pollutants from wastewaters, it is too expensive to be used practically. Therefore, there is a need to develop a low-cost adsorbent for the removal of heavy metal ions from the aqueous environment. Several types of biomasses have been explored as the alternate cases in wastewater treatment for chromium removal. The different biomasses which were tested in previous studies include corncob waste (Moreno-Pirajana et al. 2013), saw dust (Mane and Vijay-Babu 2011), coconut shell carbon (Amuda et al. 2007), tea waste (Malkoc and Nuhoglu 2006), rice hulls (Marshall and Wartelle 2004), hazelnut shell (Ayoama et al. 1999) etc.

The aim of this study is to investigate the possibility for the preparation of biochar from a weed (*Onopordom Heteracanthom*), as an alternate low-cost adsorbent material for the removal of Cr(VI) from wastewater. The impact of the initial concentration of Cr(VI), adsorbent dosage, and initial pH on the adsorption capacity were investigated. Furthermore, the adsorption isotherms and kinetics were deduced from the experimental results. This research has been conducted between December 23 and September 11 of 2013 in the laboratory of applied chemistry of Islamic Azad University, Tabriz Branch.

Materials and methods

Preparation of adsorbent

Onopordom Heteracanthom (*OH*) was obtained from the suburbs of Tabriz, Iran. *OH* is a thorn with approximately 80–120 cm of height and is among many herbs which grow beside roads and cultivated or undeveloped farms. Its seeds are used in medicinal industry, but its bough is not useful and is considered as agricultural products waste. The geographical dispersion of this plant covers all areas of Iran. Firstly, the samples were cleaned from thorns and leaves and were divided into smaller particles. The particles were milled and then were washed with deionized water until all leachable impurities were removed. Finally, the samples were dried in hot air oven at 100 °C for 4 h. Thereafter, the samples were treated with H_2SO_4 (50 %) at the ratio of 2:1 (acid volume/weight of *OH*), and they were allowed to get carbonized at 150 °C in hot air oven for 24 h

and soaked with deionized water until the pH of solution got stable. Afterward, the produced carbon was soaked in 2 % $NaHCO_3$ (w/v) till any residual acid was removed. Finally, the samples were dried in hot air oven at 110 °C, cooled, sieved in the size of 300 μm, and stored for further utilization (Kadirvelu et al. 2001). Zero point charge (ZPC) of adsorbent determined by salt addition method (Mahmood et al. 2011).

Characterization methods

The prepared adsorbent was characterized using different techniques such as Brunauer–Emmett–Teller (BET), scanning electron microscopy (SEM), Fourier transform infrared spectroscopy (FT-IR), and energy-dispersive X-ray (EDX).

Adsorption experiments

Cr(VI) solution was prepared using analytical grade of $K_2Cr_2O_7$ obtained from Merck Company and stored at room temperature. This stock solution was used to prepare dilute solutions of chromium ion by the dilution with double distilled water. The adsorption studies of Cr(VI) ions onto the adsorbent were investigated in a shaking water bath with a constant speed of 140 rpm. In each experiment a certain amount of adsorbent was mixed with 100 mL of Cr(VI) solution at a given initial concentration and pH in a fixed temperature. After mixing them, every 10 min, about 5 mL of the solution was sampled and separated from the adsorbent using filter paper. The residual amount of Cr(VI) ions in the samples was determined using UV/Vis spectrophotometer (Shimadzu, UV-1700) in the maximum wavelength of Cr(VI) (Mohapatra et al. 2005).

The effect of the initial concentration of Cr(VI) (10, 20, 30, 40, 50, 60 mg L^{-1}), dosage of adsorbent (0.1, 0.15, 0.2 g), and initial pH (1, 2, 3, 4) were investigated in this research. The adsorption yield (R %) and the amount of the adsorbed per unit of adsorbent (q_e) were calculated by Eqs. 1 and 2, respectively:

$$R\% = \frac{(C_0 - C_t)}{C_0} \times 100 \tag{1}$$

$$q_e = \frac{(C_0 - C_e) \times V}{W} \tag{2}$$

where C_0 is the initial concentration of Cr(VI) (mg L^{-1}), C_t is the concentration of Cr(VI) at any time (mg L^{-1}), C_e is the equilibrium concentration of Cr(VI) (mg L^{-1}), V is the volume of Cr(VI) solution (L) and W is the weight of the adsorbent (g).

Results and discussion

Characterization of adsorbent

Fourier transform infrared (FT-IR) was used to determine the changes of vibration frequency in the functional groups of the adsorbent due to Cr(VI) adsorption. The FT-IR spectrum within 500–4000 cm^{-1} for the biochar particles obtained from the *OH* (BCP) before and after the adsorption of Cr(VI) is shown in Fig. 1a, b.

In the case of BCP (Fig. 1a), the peak point of around 3413.17 cm^{-1} indicates the existence of free and intermolecular bonded hydroxyl groups. Also the peak position of 1622 cm^{-1} in the FT-IR spectrum of BCP can be related to the C=C bond. The additional peak at 618 cm^{-1} can be attributed to bending modes of aromatic compounds.

The FT-IR spectrum of Cr(VI) loaded BCP (Fig. 1b) indicates that there is remarkable change in the hydroxyl group peak at 3413.17 cm^{-1} which it can be due to Cr(VI) binding mostly with hydroxyl groups (Garg et al. 2007).

For determining the specific surface area, total pore volume, and pore size of BCP, BET-BJH methods were used. According to the BET method, the specific surface area and mean pore diameter was obtained as 5.73 m^2 g^{-1} and 4.5 nm, respectively. The nitrogen adsorption–desorption isotherm onto BCP is shown in Fig. 2a, which is in correspondence with classical Type III isotherm of IUPAC classification and indicates weak adsorbent-adsorbate interactions on non-porous or macroporous adsorbent (Rouquerol et al. 2013). BCP pore size distribution was determined by the BJH method. Figure 2b shows a board distribution (1–50 nm) for pore size distribution.

SEM images have been used for morphological study of BCP. The SEM micrographs of BCP before and after adsorption of Cr(VI) are shown in Fig. 3a, b, respectively. In the SEM image of BCP, the porous structure is obvious, but in the case of the used particles, the pores have been covered by the adsorbate.

The EDX spectrum of BCP before and after adsorption of Cr(VI) was evaluated. The spectrum clearly indicates the peak of element C. There is a remarkable reduction in the intensity of peak of C in the used sample (Fig. 3c), comparing with the fresh one, and also the peak of Cr(VI) is notable on the used BCP.
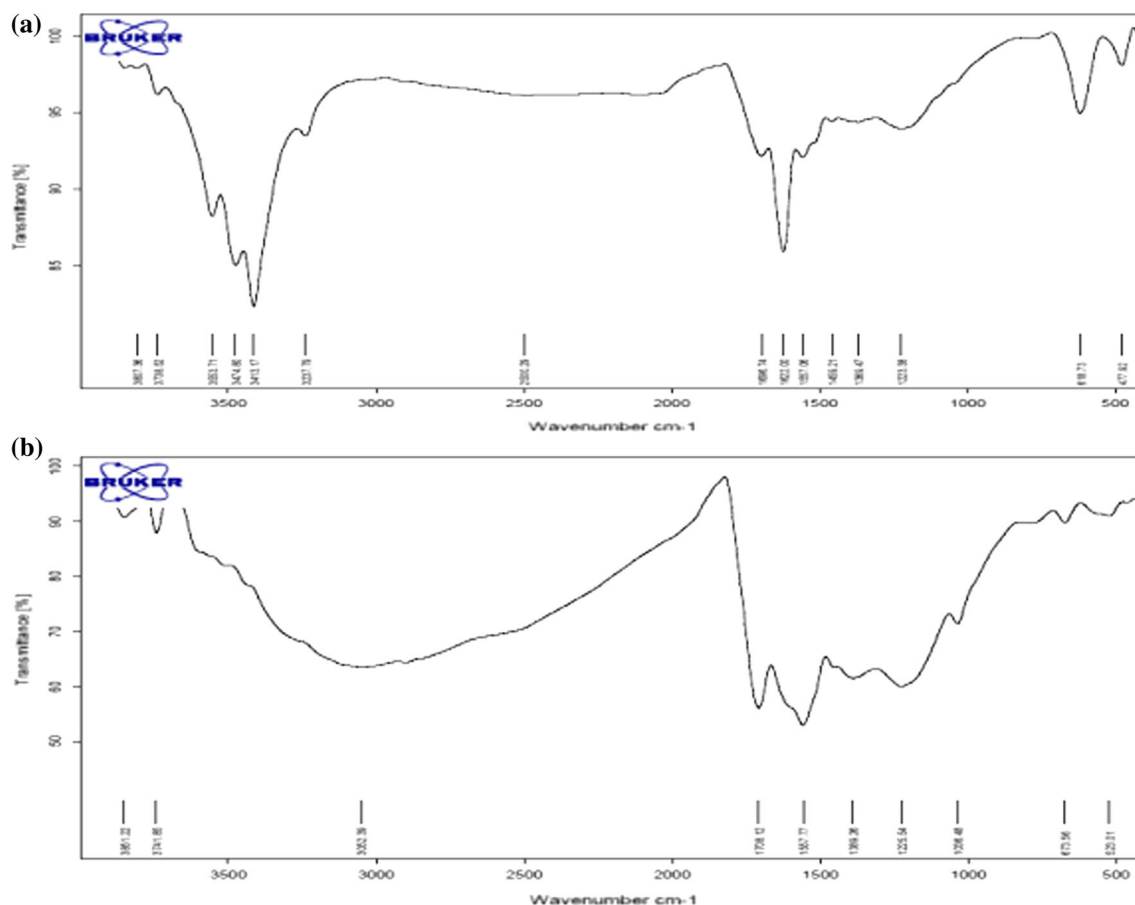

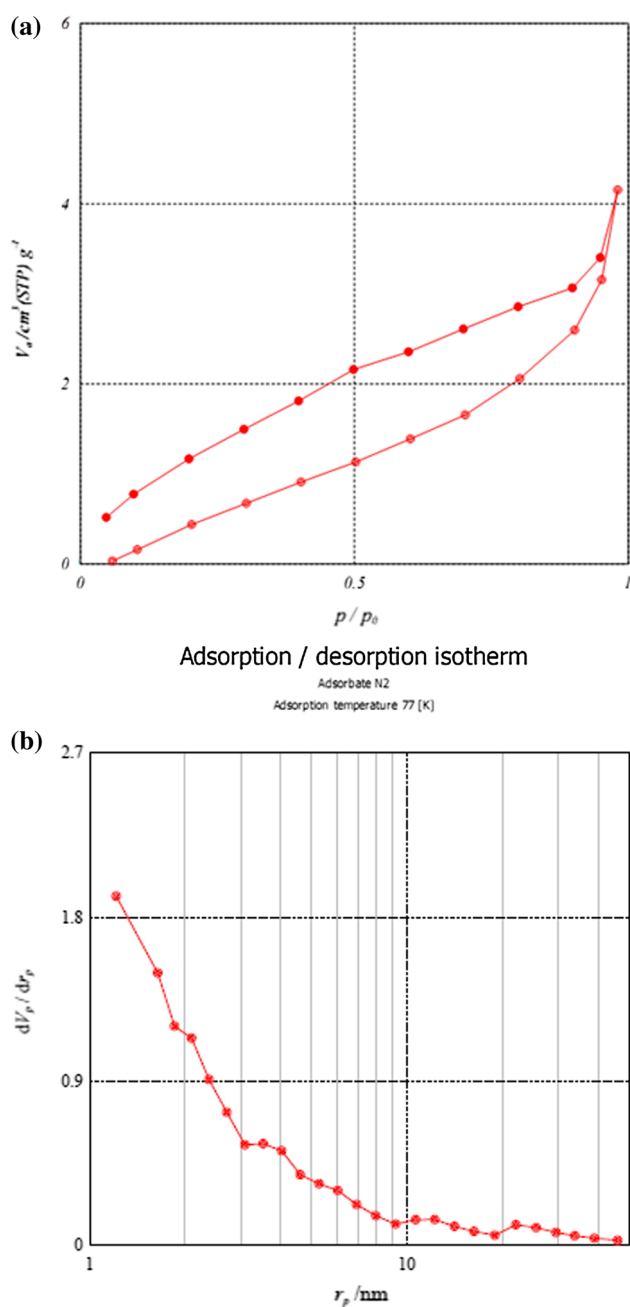**Fig. 1** FT-IR spectrum of BCP before (**a**) and after adsorption of Cr(VI) (**b**)

1806

Int. J. Environ. Sci. Technol. (2016) 13:1803–1814

(a)

Adsorption / desorption isotherm
Adsorbate N2
Adsorption temperature 77 [K]

(b)

Fig. 2 Nitrogen adsorption–desorption isotherm (**a**) and BJH pore size distribution of BCP (**b**)

Adsorption studies

The effect of the initial concentration of Cr(VI)

One of the most important parameters that influence adsorption process is the initial concentration of adsorbate. Therefore, the effect of the initial concentration of Cr(VI) was studied by performing the experiments at different initial concentrations (10, 20, 30, 40, 50 and 60 mg L^{-1}) keeping pH (2.0), adsorbent dose (0.1 g), stirring speed (140 rpm), and temperature (15 $\pm$ 1 °C) constant. The results of this study are shown in Fig. 4a. This diagram indicated that the percentage of adsorption decreased by increasing the initial concentration of Cr(VI); it is apparent that the adsorbent had a limited number of active sites, and these sites were saturated in a certain concentration, so the saturated adsorbent would not be able to uptake more Cr(VI) molecules (Chowdhury et al. 2011).

The results in Fig. 4b indicate that the capacity of adsorbent increased by increasing the initial concentration of Cr(VI). The increase in concentration can provide a driving force to overcome all-mass transfer resistances from aqueous to solid phase (Chowdhury et al. 2011).

The effect of BCP dosage

The effect of BCP dosage on the adsorption of Cr(VI) from aqueous solutions was evaluated. Figure 5a shows the effect of BCP dosage on the adsorption capability of Cr(VI). Increasing the adsorption efficiency by increasing adsorbent dosage was due to the availability of greater surface area and adsorption sites for the constant number of Cr(VI) ions (Rasoulifard et al. 2010).

Figure 5b indicates that by increasing the adsorbent dosage from 0.1 to 0.2 g, the value of q_{eq} also decreases. This reduction may be attributed to unsaturation of adsorption sites and also increase in diffusionpath length resulting from aggregation of BCP particles (Behnajady and Bimeghdar 2014).

The effect of initial pH

The effect of pH on the adsorption of Cr(VI) from aqueous environments onto BCP has been investigated. This parameter influences both the chemical state of Cr(VI) and the surface charge of adsorbent. The adsorption percentage of Cr(VI) onto BCP as a function of pH was studied. By increasing pH, the percentage of Cr(VI) adsorption decreases. The adsorption percentage of Cr(VI) onto BCP was 88, 69, 6 and 0.5 % for the pH values of 1, 2, 3 and 4, respectively. The pH of zero point charge for adsorbent (pHzpc) is 2 and as we know the surface charge is neutral at pHzpc. For lower pH values (pH below pHzpc), the surface of adsorbent is covered by H$^+$ ions and has a positive electrical load, while at higher ones the adsorbent surface involves negative electrical load. Consequently, at lower pH values it is easier for dichromate ion to load onto adsorbent (Gupta and Babu 2009).
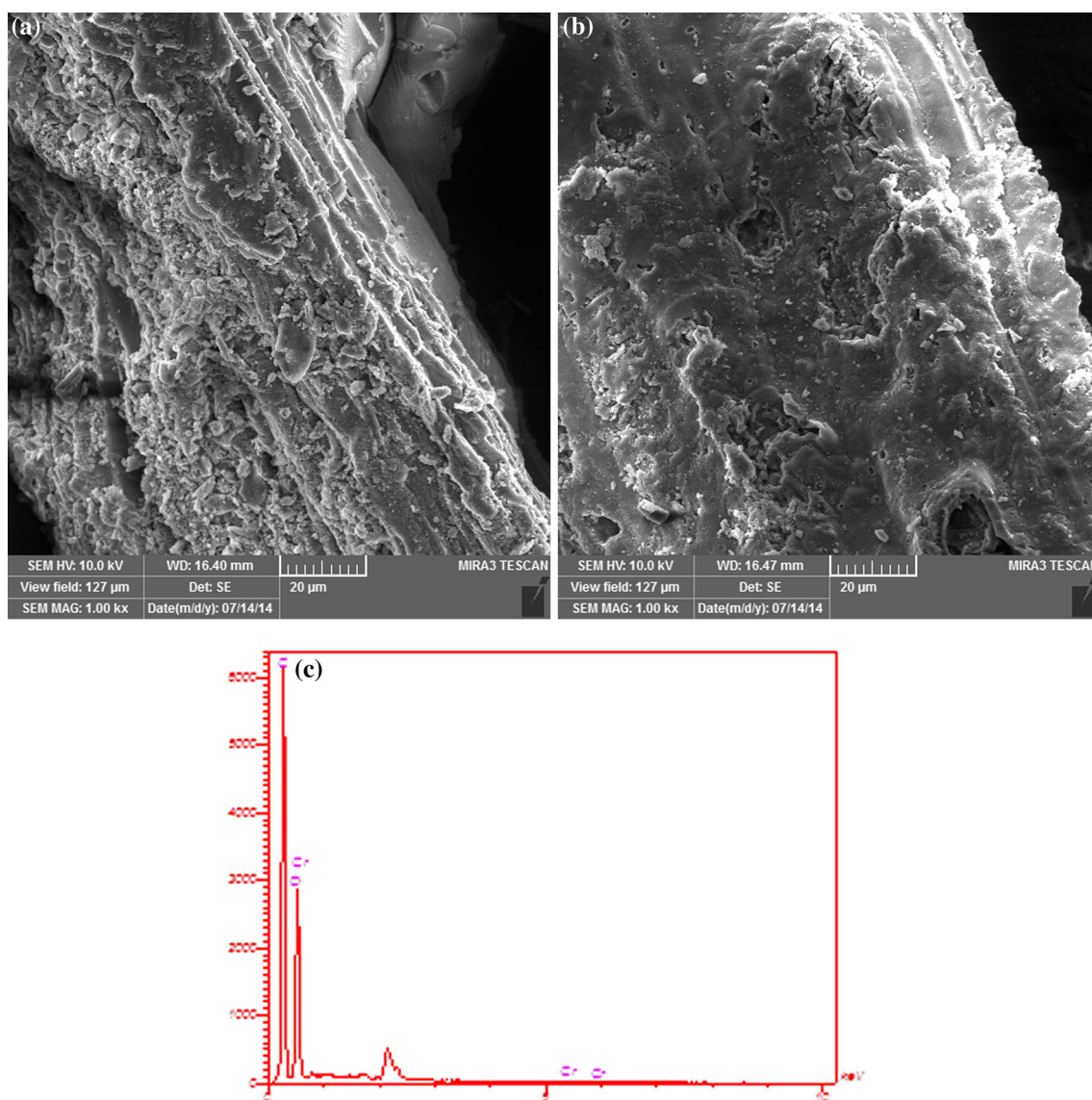
Fig. 3 The SEM image of BCP before (**a**) and after adsorption of Cr(VI) (**b**), EDX spectrum of BCP after adsorption of Cr(VI) (**c**)

Equilibrium isotherm studies

The adsorption isotherm explains the way of interactions between adsorbent and adsorbate. Therefore, it is always considered as a major factor for determining the adsorbent capacity and optimizing adsorbent consumption. In this condition, the distribution of solute between solution and adsorbent surface is expressed as a function of C_e and q_e at a constant temperature called equilibrium adsorption isotherm (Kundu and Gupta 2006).

Several 2 and 3-parameters isotherm models have been used in this study. The isotherm parameters were evaluated by nonlinear trial and error method using Polymath 6.0 software. As the higher values of correlation coefficient (R^2) and adjusted correlation coefficient (R^2_{adj}), it can be concluded that the data are in a better agreement with the mentioned model. The average values of observations ($\bar{y}$), R^2 and R^2_{adj} were calculated by Eqs. 3–5, respectively:

$$\bar{y} = \frac{1}{n}\left(\sum_{i=1}^{n} y_{i_{\text{obs.}}}\right) \tag{3}$$

$$R^2 = 1 - \frac{\sum_{i=1}^{n}\left(y_{i_{\text{obs.}}} - y_{i_{\text{calc.}}}\right)^2}{\sum_{i=1}^{n}\left(y_{i_{\text{obs.}}} - \bar{y}\right)^2} \tag{4}$$
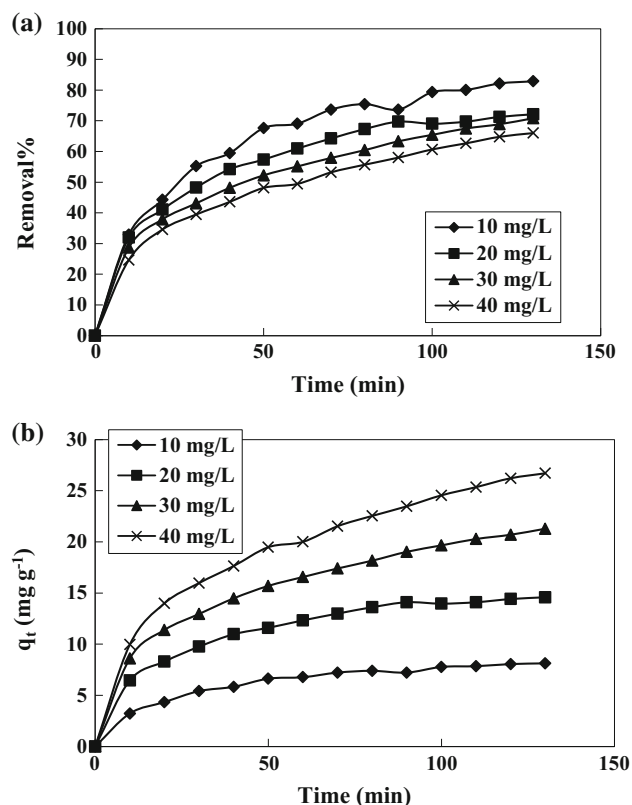
Fig. 4 Effect of initial Cr(VI) concentration on the adsorption percent of Cr(VI) onto BCP (**a**) and q_eq (**b**) (BCP = 0.1 g, pH = 2, $T = 15 \pm 1\ ^\circ C$)

Fig. 5 Effect of initial dosage of BCP on the adsorption percent of Cr(VI) onto BCP (**a**) and q_eq (**b**) ([Cr]$_0$ = 20 mg L^{-1}, pH = 2, $T = 15 \pm 1\ ^\circ C$)

$$R^2_{\text{adj.}} = 1 - \frac{(1 - R^2)(n - 1)}{n - p} \qquad (5)$$

where n is the number of observations, y_i is a specific observation, the notation "obs." relates to the observed data and notation "calc." relates to the calculated data. For comparing the various isotherm models in adsorption of Cr(VI) by BCP, we have also used variance (S^2) and root-mean-square error (Rmse) parameters. A model with smaller variance and Rmse shows the data accurately. To calculate the values of Rmse and S^2, Eqs. 6 and 7 have been used, respectively.

$$\text{Rmse} = \frac{1}{n}\left(\sum_{i=1}^{n}\left(y_{i_{\text{obs.}}} - y_{i_{\text{calc.}}}\right)^2\right)^2 \qquad (6)$$

$$S^2 = \frac{\sum_{i=1}^{n}(y_i - \bar{y})^2}{n - 1} \qquad (7)$$

The parameters of each model at 95 % confidence interval, R^2, $R^2_{\text{adj.}}$, S^2 and Rmse were calculated and are given in Table 1. For the regression model to be stable and statistically valid, the confidence intervals must be much
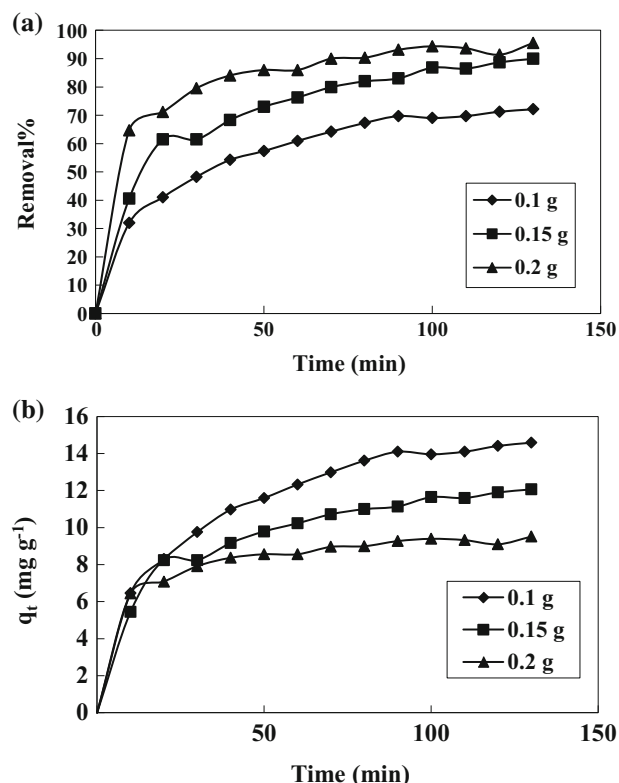
smaller (or at least smaller) than the respective parameter values (in absolute values). The curves of experimental data and the results obtained from different 2 and 3 parameters models are shown in Fig. 6a, b, respectively.

Langmuir isotherm

Langmuir model is the most practical and known type of adsorbent isotherm which is in a good agreement with a wide range of experimental data. In the lower concentrations, this equation is converted to the Henry's model (Ho et al. 2001).

The assumptions of Langmuir isotherm can be considered as single layer of adsorption, adsorption in the homogenous sites, homogenous structure of the adsorbent and limited capacity for the adsorption. This isotherm model can be expressed using the following equation:

$$q_e = \frac{q_m K_L C_e}{1 + K_L C_e} \qquad (8)$$

where C_e is the equilibrium concentration of solute (mg L^{-1}), q_e is the amount of adsorbate adsorbed at equilibrium

Table 1 Isotherm and kinetics models parameters values (± 95% confidence level)

Model	R^2	R^2_{adj}	S^2	Rmse	Parameters	Parameter values
Two- and three- parameter isotherm models						
2-p Langmuir	0.9795497	0.9754597	2.962681	0.5498312	q_m, K_L	37.28(± 8.17), 0.13(± 0.08)
2-p Freundlich	0.9690305	0.9628367	4.48662	0.9766227	K_F, n	7.52(± 1.0002), 2.38(± 6.26)
2-p Temkin	0.976497	0.9717964	3.404935	0.5894424	q_m	15.80(± 0.0005)
					RT/ $(-\Delta H^0_{ad})$	0.50(± 0.0001)
					K_T	1.42(± 0.0001)
3-p Redlich-Peterson	0.9797579	0.9696369	3.66565	0.5470254	A	5.42(± 2.56)
					B	0.18(± 0.19)
					g	0.93(± 0.22)
3-p Sips	0.9801056	0.9701584	3.602684	0.5423068	q_m	40.54(± 35.61)
					K_a	0.10(± 0.23)
					α	0.10(± 0.23)
3-p Toth	0.9797579	0.9696369	3.66565	0.5470254	q_m	35.29(± 0.001)
					K_{Th}	0.16(± 1.43)
					β	0.93(± 5.74)
Kinetics models						
Pseudo-first- order ($[Cr]_0 = 20$ mg L^{-1})	0.977656	0.975794	0.4004096	0.1565723	q_e	14.11(± 0.62)
					k_1	0.04(± 0.007)
Pseudo-second- order ($[Cr]_0 = 20$ mg L^{-1})	0.9940189	0.9935205	0.1071818	0.0810071	q_e	16.65(± 0.17)
					k_2	0.003(± 0.0001)
Pseudo-first- order ($[Cr]_0 = 40$ mg L^{-1})	0.9649254	0.9620025	2.04934	0.3542172	q_e	25.42 (± 0.0003)
					k_1	0.032(± 1.4E − 06)
Pseudo-second- order ($[Cr]_0 = 40$ mg L^{-1})	0.9862294	0.9850819	0.8045881	0.2219471	q_e	31.0846(± 0.19)
					k_2	0.001(± 3.06E − 05)

(mg g^{-1}), q_m is the maximum adsorption capacity and K_L is the Langmuir adsorption model constant (L mg^{-1}). The obtained R^2 value for this model ($R^2 = 0.979$) indicates that adsorption of Cr(VI) from aqueous solutions by BCP is based on this model. The maximum adsorption capacity (q_m) obtained from Langmuir isotherm is 37.28 mg g^{-1}. Table 2 lists maximum capacity of the mono-layer adsorption of BCP and other adsorbents reported in the literature. In general prepared adsorbent in this work exhibited satisfactory adsorption capacity in comparison with other similar adsorbents.

Considering the separation factor for different initial Cr(VI) concentrations, it can be asserted that in all initial concentrations, the adsorption of Cr(VI) is favorable.

Freundlich isotherm

The Freundlich isotherm equation is an empirical equation and is used for studying experimental data in liquid phase. This isotherm is used for describing the multilayer adsorption with the reaction among the adsorbed molecules and also is effective for adsorption on the heterogeneous surfaces (Gimbert et al. 2008; Oubagaranadin and Murthy 2009). This isotherm is an exponential equation with the assumption that by increasing the concentration of the adsorbed mass, there is more amount of adsorption. From theoretical point of view, using this equation can result in unlimited amount of adsorption (Allen et al. 2004). The Freundlich equation can be expressed as follows:

$$q_e = K_F C_e^{\frac{1}{n}} \tag{9}$$

where K_F is Freundlich adsorption model constant (L g^{-1}) and shows the quantity of adsorbate adsorbed onto the adsorbent for a unit equilibrium concentration, and n is Freundlich adsorption model exponent. When the $1/n$ is equal to 1, the adsorption is linear. For the values less than 1, the adsorption process is chemical, and if it is more than one, the adsorption will be a physical process. The most surface heterogeneity occurs when the value of 1/n is near to zero (Gimbert et al. 2008).

1810

Int. J. Environ. Sci. Technol. (2016) 13:1803–1814
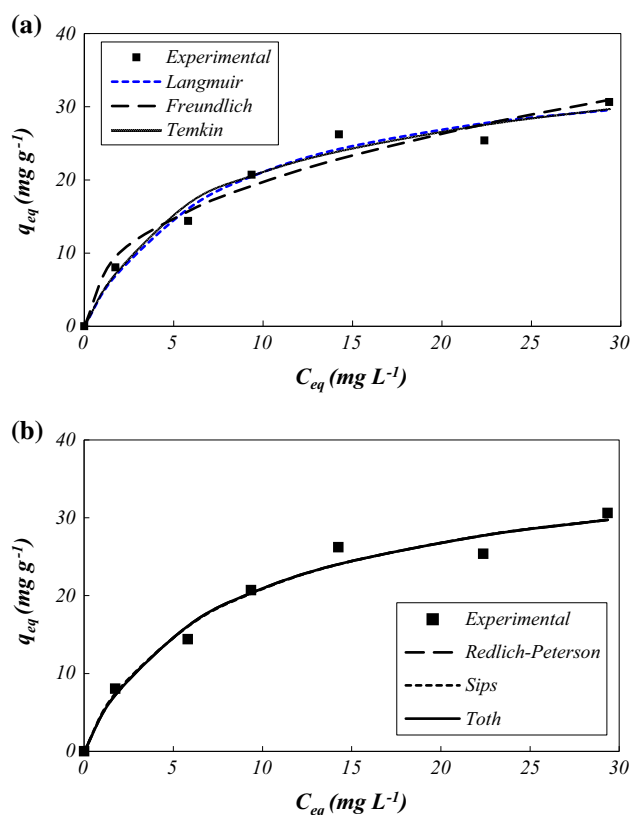
(a)

(b)

Fig. 6 Comparison of 2-parameters isotherm models (a) and 3-parameters isotherm models (b) for adsorption of Cr(VI) from the aqueous solutions onto BCP with experimental results (BCP = 0.1 g, pH = 2, $T = 15 \pm 1$ °C)

According to the results in Table 1, the n value obtained from Freundlich model is above unity, indicate favorable adsorption conditions; however, the R^2 value for this isotherm is not close enough to 1 and shows that the Langmuir model provided a good fit to the experimental data when compared with the Freundlich model.

Temkin isotherm

Temkin isotherm is based on the assumption that due to the interaction between adsorbent-adsorbate, the heat of adsorption of all molecules in a certain layer decreases linearly with surface coverage (Samarghandi et al. 2009). This model can be expressed in the following equation:

$$q_e = q_m \frac{RT}{(-\Delta H_{ad}^0)} \ln(K_T C_e) \quad (10)$$

where T is absolute temperature (K), R is universal gas constant (J mol^{-1} K^{-1}), K_T is Temkin model constant (L mg^{-1}) and $-\Delta H_{ad}^0$ is the heat of adsorption (J mol^{-1}). This model gives a satisfactory fit to the experimental data. For adsorption heat lower than 8 kJ mol^{-1}, physisorption plays a significant role in the adsorption mechanism. The low value of the adsorption heat ($-\Delta H_{ad}^0 = 4.77$ kJ mol^{-1}) in this work, confirmed the physical adsorption of Cr(VI) by BCP.

Redlich–Peterson isotherm

The Redlich–Peterson equation is used as a comparison between Langmuir and Freundlich isotherms. This equation at the higher concentrations of adsorbate is converted to the Freundlich isotherms and because of its multifunctional property, it can be used in either homogenous or heterogeneous systems (Gimbert et al. 2008; Subramanyam and Das 2009). Redlich–Peterson isotherm can be described as follows:

$$q_e = \frac{A C_e}{1 + B C_e^g} \quad (11)$$

where A and B are Redlich–Peterson model constants, and g is Redlich–Peterson model exponent. When g is equal to 1, the Redlich-Peterson equation is converted to Langmuir

Table 2 Maximum adsorption capacity of BCP compared to the other adsorbents in the adsorption of Cr(VI)

Adsorbent	pH	q_m (mg g^{-1})	References
FAC (Activated carbon derived from coconut fibers)	2	21.75	Mohan et al. (2005)
SAC (Activated carbon derived from coconut shells)	2	9.53	Mohan et al. (2005)
Activated carbon fabric cloth	2	22.29	Mohan et al. (2005)
CSC (Coconut shell charcoal oxidized with nitric acid)	4	10.88	Babel and Kurniawan (2004)
CAC (Commercial activated carbon oxidized with nitric acid)	6	15.47	Babel and Kurniawan (2004)
Carbon slurry	2	15.24	Gupta et al. (2010)
Granular activated carbon (Merck)	6.5	3.9	Rivera-Utrilla et al. (2003)
Granular activated carbon (Merck) modified with the bacteria	6.5	3.3	Rivera-Utrilla et al. (2003)
BCP	2	37.28	This work

and in the case of $g = 0$, it is converted to Henrys' equation. According to the obtained value for g (0.93), it is obvious that the adsorption of Cr(VI) onto BCP mainly follows Langmuir isotherm.

Sips isotherm

In fact, the Sips isotherm is a composition of Langmuir and Freundlich isotherms which follows the Freundlich and Langmuir at the lower and higher adsorption concentrations, respectively. This isotherm predicts a single layer capacity of adsorption at the higher adsorption concentrations (Oubagaranadin and Murthy 2009; Subramanyam and Das 2009). The equation of Sips isotherm can be described using the following formula:

$$q_e = \frac{q_m (K_a C_e)^\alpha}{1 + (K_a C_e)^\alpha} \tag{12}$$

where K_a is Sips model constant (L mg^{-1}), and α is Sips model exponent; this indicates the heterogeneity of system. According to the Table 1, the Sips isotherm fits adequately the experimental data. The α value is close to 1 and indicates that the adsorption process is mainly Langmuir form.

Toth isotherm

Toth isotherm model was derived from potential theory and is useful to describe the sorption process in heterogeneous systems. This model assumes an asymmetrical quasi-Gaussian energy distribution. According to this model, most sites have sorption energy less than the mean value of adsorption energy. This isotherm is converted to the Langmuir isotherm when β is equal 1 (Allen et al. 2003; Oubagaranadin and Murthy 2009). Toth isotherm can be expressed using the following equation:

$$q_e = \frac{q_m K_{TH} C_e}{[1 + (K_{TH} C_e)^\beta]^{1/\beta}} \tag{13}$$

where K_{Th} is Toth model constant (L mg^{-1}) and β is Toth model exponent. According to the results in Table 1, the β value obtained for our adsorption process is close to 1 ($\beta = 0.93$), so we can conclude that the adsorption of Cr(VI) onto BCP has good conformity with Langmuir isotherm.

Adsorption kinetic studies

Studying of adsorption kinetics is one of the most important investigations of adsorption process. Adsorption kinetic depends on the physical and chemical properties of adsorbent which influences the adsorption mechanism. Kinetic models are used to indicate the adsorption mechanism and final controlling steps (Ho and McKay 1999a). In order to understand the kinetics of Cr(VI) adsorption onto BCP as an adsorbent, pseudo-first-order and pseudo-second-order kinetic models are tested with the experimental data.

Lagergren's pseudo-first-order kinetic model

This model has been proposed by Lagergren and described as the below formula (Lagergren 1898):

$$q_t = q_e (1 - e^{-k_1 t}) \tag{14}$$

where q_e and q_t are the amount of adsorbate adsorbed at equilibrium and at any time (mg g^{-1}), respectively, and k_1 is the first-order Lagergren model rate constant (min^{-1}).
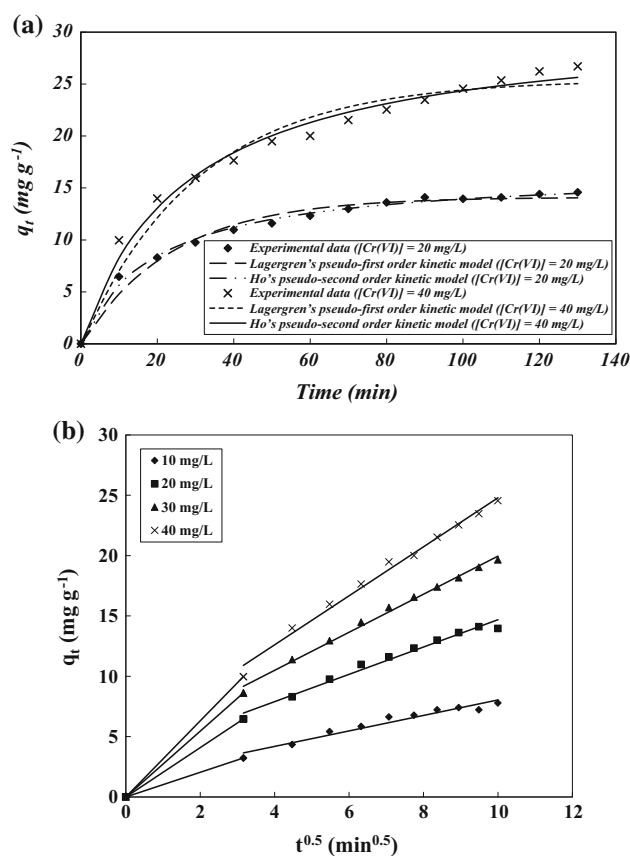

Fig. 7 Comparison of kinetic models with experimental results (**a**) and Weber–Morris kinetic model (**b**) for adsorption of Cr(VI) from aqueous solutions by BCP (Ads = 0.1 g, pH = 2, $T = 15 \pm 1\ ^\circ C$)

1812

Int. J. Environ. Sci. Technol. (2016) 13:1803–1814

Ho's pseudo-second-order kinetic model

The Ho's pseudo-second-order kinetic model is described in the following way (Ho and McKay 1999b):

$$q_t = \frac{q_e^2 k_2 t}{1 + k_2 q_e t} \tag{15}$$

where k_2 is Ho pseudo-second-order kinetic model rate constant (g mg^{-1} min^{-1}).

The values of k_1, k_2 and q_e are given in Table 1. The results in Table 1 and Fig. 7a show that Cr(VI) adsorption onto BCP has very good compliance with pseudo-second-order kinetic model. The value of R^2 is greater than 0.99 and also, S^2 and Rmse are very close to zero. According to this model, two reactions occur, the first one is fast and reaches equilibrium quickly, and the second is slow that can continue for a long time (Behnajady et al. 2014; Mody et al. 2009).

The mechanism of adsorption

The intra-particle diffusion or Weber and Morris adsorption kinetic model was used to describe the mechanism of adsorption process (Weber and Morris 1963). This model is described as below:

$$q = k_{ip} t^{0.5} + C_i \tag{16}$$

where k_{ip} is intra-particle diffusion kinetic model rate constant (mg g^{-1} min$^{-0.5}$), and C_i is the intercept of stage i which estimates the thickness of the boundary layer. According to this model, a linear plot indicates a rate controlled by intra-particle diffusion (Gad and El-Sayed 2009). Figure 7b indicates that the adsorption process of the Cr(VI) onto BCP is comprised of two stages. At the first stage ($t < 10$ min), a very fast adsorption is observed. The first stage of the plot indicated a fast adsorption of Cr(VI) onto the available external surface of adsorbent (boundary layer diffusion), whereas the second linear stage is due to intra-particle diffusion (Oubagaranadin and Murthy 2009). In this stage, the adsorption of Cr(VI) molecules occurs onto the active sites of the adsorbent internal surface. The intercept of the second stage lines provide an estimate of the thickness of the boundary layer. The larger intercept value indicates the greater boundary layer effect. The increase in Cr(VI) initial concentration causes an increase in the driving force and diffusion rate (Dogan et al. 2009). According to the results in Table 3, the values of intercept was found to increase with an increase in the initial Cr(VI) concentration, which indicated an increase in the thickness of the boundary layer and higher contribution of the surface adsorption in the rate-limiting

Table 3 Weber–Morris kinetic model parameters values

Cr(VI) initial concentration (mg L^{-1})	K_{ip}	C_i	R^2
10	0.642	1.621	0.953
20	1.132	3.363	0.981
30	1.579	4.177	0.993
40	2.033	4.471	0.990

step (Dogan et al. 2009). The slope of the second linear stage of the plot has been considered as the intra-particle diffusion rate constant (k_{ip}). The multi-linearity plot indicates that the intra-particle diffusion is not merely the rate-controlling step for the whole adsorption process (Oubagaranadin and Murthy 2009).

Conclusion

In this work, the biochar particles obtained from the *OH* (BCP) was used as an alternative adsorbent for the removal of Cr(VI) from aqueous solution. The morphology and purity of BCP have been studied by SEM and EDX, respectively. The BET technique was used to evaluate the specific surface area of these particles and their pores and holes. As a result, the specific surface area is about 5.73 m^2 g^{-1}. The results confirm that the BCP is an efficient adsorbent for the removal of Cr(VI) from aqueous environments. The effect of various parameters such as the initial concentration of Cr(VI), the amount of adsorbent, and pH is investigated. The most proper pH value for this process was revealed as pH = 1. Various nonlinear isotherm models were evaluated, and the results proposed the Langmuir isotherm as the best and the most proper one for confirming the experimental data for this process. Studying nonlinear kinetic equations indicates that the removal adsorption process of Cr(VI) onto BCP follows Ho's pseudo-second-order kinetic model.

References

Aliabadi M, Morshedzadeh K, Soheyli H (2006) Removal of hexavalent chromium from aqueous solution by lignocellulosic solid wastes. Int J Environ Sci Technol 3:321–325

Allen SJ, Gan Q, Matthews R, Johnson PA (2003) Comparison of optimised isotherm models for basic dye adsorption by kudzu. Bioresour Technol 88:143–152

Allen SJ, Mckay G, Porter JF (2004) Adsorption isotherm models for basic dye adsorption by peat in single and binary component systems. J Colloid Interface Sci 280:322–333

Amuda OS, Giwa AA, Bello IA (2007) Removal of heavy metal from industrial wastewater using modified activated coconut shell carbon. Biochem Eng J 36:174–181

An Z, Zhang H, Wen Q, Chen Z, Du M (2014) Desalination combined with hexavalent chromium reduction in a microbial desalination cell. Desalination 354:181–188

Ayoama M, Sugiyama T, Doi S, Cho NS, Kim HE (1999) Removal of hexavalent chromium from dilute aqueous solution by coniferous leaves. Holzforschung 53:365–368

Bailey SE, Olin TJ, Bricka RM, Adrian DD (1999) A review of potentially low-cost sorbents for heavy metals. Water Res 33:2469–2479

Behnajady MA, Bimeghdar S (2014) Synthesis of mesoporous NiO nanoparticles and their application in the adsorption of Cr(VI). Chem Eng J 239:105–113

Behnajady MA, Mansoriieh N, Modirshahla N, Shokri M (2012) Influence of operational parameters and kinetics analysis on the photocatalytic reduction of Cr(VI) by immobilized ZnO. Environ Technol 33:265–271

Behnajady MA, Yavari SH, Modirshahla N (2014) Investigation adsorption capacity of TiO_2-P25 nanoparticles in the removal of a mono-azo dye from aqueous solution: a comprehensive isotherm analysis. Chem Ind Chem Eng Q 20:97–107

Bhowal A, Bhattacharyya G, Inturu B, Datta S (2012) Continuous removal of hexavalent chromium by emulsion liquid membrane in a modified spray column. Sep Purif Technol 99:69–76

Chowdhury S, Mishra R, Saha P, Kushwaha P (2011) Adsorption thermodynamics, kinetics and isosteric heat of adsorption of malachite green onto chemically modified rice husk. Desalination 265:159–168

Chun L, Hongzhang C, Zuoho L (2004) Adsorptive removal of Cr(VI) by Fe-modified steam exploded wheat straw. Proc Biochem 39:541–545

Das N, Vinodhini V (2010) Packed bed column studies on Cr(VI) removal from tannery wastewater by neem sawdust. Desalination 264:9–14

Dogan M, Abak H, Alkan M (2009) Adsorption of methylene blue onto hazelnut shell: kinetics, mechanism and activation parameters. J Hazard Mater 164:172–181

Gad HMH, El-Sayed AA (2009) Activated carbon from agricultural by-products for the removal of Rhodamine-B from aqueous solution. J Hazard Mater 168:1070–1081

Garg UK, Kaur MP, Garg VK, Sud D (2007) Removal of hexavalent chromium from aqueous solution by agricultural waste biomass. J Hazard Mater 140:60–68

Gimbert F, Morin-Crini N, Renault F, Badot PM, Crini G (2008) Adsorption isotherm models for dye removal by cationized starch-based material in a single component system: error analysis. J Hazard Mater 157:34–46

Gode F, Atalay ED, Pehlivan E (2008) Removal of Cr(VI) from aqueous solutions using modified red pine sawdust. J Hazard Mater 152:1201–1207

Gupta S, Babu BV (2009) Removal of toxic metal Cr(VI) from aqueous solutions using sawdust as adsorbent: equilibrium, kinetics and regeneration studies. Chem Eng J 150:352–365

Ho YS, McKay G (1999a) Comparative sorption kinetic studies of dyes and aromatic compounds onto fly ash. J Environ Sci Health A 34:1179–1204

Ho YS, McKay G (1999b) Pseudo-second order model for sorption processes. Process Biochem 34:451–465

Ho YS, Porter JF, Mckay G (2001) Equilibrium isotherm studies for the sorption of divalent metal ions onto peat: copper, nickel and lead single component systems. Water Air Soil Pollut 141:1–33

Hu J, Chen G, Lo IMC (2005) Removal and recovery of Cr(VI) from wastewater by maghemite nanoparticles. Water Res 39:4528–4536

Kadirvelu K, Thamaraiselvi K, Namasivayam C (2001) Adsorption of nickel(II) from aqueous solution onto activated carbon prepared from coirpith. Sep Purif Technol 24:497–505

Kotas J, Stasicka Z (2000) Chromium occurrence in the environment and methods of its speciation. Environ Pollut 107:263–283

Kundu S, Gupta AK (2006) Arsenic adsorption onto iron oxide-coated cement (IOCC): regression analysis of equilibrium data with several isotherm models and their optimization. Chem Eng J 122:93–106

Lagergren S (1898) Zur theorie der sogenannten adsorption geloster stoffe. K seven Vetenskapsakad Handl 24:1–39

Mahmood T, Saddique MT, Naeem A, Westerhoff P, Mustafa S, Alum A (2011) Comparison of different methods for the point of zero charge determination of NiO. Ind Eng Chem Res 17:10017–10023

Malkoc E, Nuhoglu Y (2006) Fixed bed studies for the sorption of chromium(VI) onto tea factory waste. Chem Eng Sci 61:4363–4372

Mane VS, Vijay- Babu PV (2011) Studies on the adsorption of Brilliant Green dye from aqueous solution onto low-cost NaOH treated saw dust. Desalination 273:321–329

Marshall WE, Wartelle LH (2004) An anion exchange resin from soybean hulls. J Chem Technol Biotechnol 79:1286

Mody K, Khambhaty Y, Basha Sh, Jha B (2009) Kinetics, equilibrium and thermodynamic studies on biosorption of hexavalent chromium by dead fungal biomass of marine Aspergillus niger. Chem Eng J 145:489–495

Mohapatra P, Samantaray SK, Parida K (2005) Photocatalytic reduction of hexavalent chromium in aqueous solution over sulphate modified titania. J Photochem Photobiol A 170:189–194

Moreno-Pirajan JC, Fonseca-Correa R, Giraldo L (2013) Trivalent chromium removal from aqueous solution with physically and chemically modified corncob waste. J Anal Appl Pyrolysis 101:132–141

Oubagaranadin JUK, Murthy ZVP (2009) Modeling of adsorption of chromium (VI) on activated carbons derived from corn (Zea mays) cob. Chem Prod Process Model 4 Article 32, doi: 10.2202/1934-2659.1377

Rasoulifard MH, Esfahlani FH, Mehrizadeh H, Sehati N (2010) Removal of C.I. basic yellow 2 from aqueous solution by low-cost adsorbent: hardened paste of Portland cement. Environ Technol 31:277–284

Rivera-Utrilla J, Bautista-Toledo I, Ferro-García MA, Moreno-Castilla C (2003) Bioadsorption of Pb(II), Cd(II), and Cr(VI) on activated carbon from aqueous solutions. Carbon 41:323–330

Rouquerol J, Rouquerol F, Llewellyn P, Maurin G, Sing KSW (2013) Adsorption by powders and porous solids, principles, methodology and applications, 2nd edn. Academic Press, Cambridge

Samarghandi MR, Hadi M, Moayedi S, Barjasteh Askari F (2009) Two-parameter isotherms of methyl orange sorption by pinecone derived activated carbon. Iran J Environ Health Sci Eng 6:285–294

1814

Int. J. Environ. Sci. Technol. (2016) 13:1803–1814

Subramanyam B, Das A (2009) Study of the adsorption of phenol by two soils based on kinetic and isotherm modeling analyses. Desalination 249:914–921

Venkateswaran P, Palanivelu K (2004) Solvent extraction of hexavalent chromium with tetrabutyl ammonium bromide from aqueous solution. Sep Purif Technol 40:279–284

Weber WJ, Morris JC (1963) Kinetics of adsorption on carbon from solution. J Sanit Eng Div Am Soc Civ Eng 89:31–60

Zongo I, Leclerc JP, Amadou-Maiga H, Wethe J, Lapicque F (2009) Removal of hexavalent chromium from industrial wastewater by electrocoagulation: a comprehensive comparison of aluminium and iron electrodes. Sep Purif Technol 66:159–166